Journal of Plant Pathology (2025) 107:795–810
https://doi.org/10.1007/s42161-024-01798-7

ORIGINAL ARTICLE

Ceratocystis cacaofunesta is responsible of cocoa crops wilt in Colombia: morphological and molecular characterization of isolates

Martha Liliana Carrero-Gutiérrez[1,3] · Sandra González-Sayer[2] · Yeirme Jaimes-Suárez[4] · Carolina González-Almario[1] · Adriana González-Almario[3]

Received: 15 May 2024 / Accepted: 29 October 2024 / Published online: 24 December 2024

Abstract
Cocoa phytosanitary problems in Colombia are one of the main causes of the decline in cocoa production, with losses that can reach 100% due to inadequate management. *Ceratocystis* wilt is a prevalent disease affecting cocoa crops in the country, with *C. fimbriata* identified as its causal agent. However, there are still inconsistencies at the morphological level regarding the causal species, which contradict the causal relationship of the pathogen with the disease, affecting its diagnosis. Studies based on the phenotypic and genotypic characterization of *Ceratocystis* species are imperative for reliable identification of the pathogen. The objective of this study was to morphologically and molecularly characterize isolates of *Ceratocystis* spp. obtained from symptomatic samples in the cocoa-producing regions of Colombia. Morphological characteristics were evaluated at the macro and microscopic levels. Additionally, isolates were identified at the species level through multi-locus analysis and phylogenetic characterization using the β-tubulin (*βT-1*), guanine nucleotide-binding protein (*MS204*), second largest subunit of RNA polymerase II (*RPBII*), and 60 S ribosomal protein L37 (*FG1093*) gene regions. The results revealed variations in the colony development and microscopic morphology. Molecular and phylogenetic analyses consistently classified all isolates as *Ceratocystis cacaofunesta*, confirming that this species is the causal agent of cocoa *Ceratocystis* wilt in Colombia.

Keywords *Ceratocystis Cacaofunesta* · *Theobroma cacao* L · *Ceratocystis* wilt · Polyphasic characterization · Multilocus analysis

Introduction

Cocoa (*Theobroma cacao* L.) a crucial tropical crop that serves as the primary source of raw materials for chocolate and confectionery production, as well as for pharmaceuticals and cosmetic products (Reyes et al. 2023). In 2017, global cocoa production reached an estimated 4.7 million metric tons annually, with the majority originating from countries across Africa, Latin America and Asia (Marelli et al. 2019; Cabrera et al. 2016). In Latin America and the Caribbean, cocoa is classified as a commercial alternative with more than 1.8 million hectares available for production (Diaz-Valderrama et al. 2020; Fontagro 2020) and constitutes the primary source of livelihood for small-scale

✉ Adriana González-Almario
adgonzalezal@unal.edu.co

✉ Martha Liliana Carrero-Gutiérrez
mcarrero@unal.edu.co

Sandra González-Sayer
smgonzalezs@unal.edu.co

Yeirme Jaimes-Suárez
yjaimes@agrosavia.co

Carolina González-Almario
cgonzaleza@agrosavia.co

[1] Centro de Investigación Tibaitatá, Corporación Colombiana de Investigación Agropecuaria-Agrosavia, Km 14 vía Mosquera-Bogotá, Cundinamarca, Colombia

[2] Laboratory of Evolutionary Genetics, Neuchâtel University, Neuchâtel, Switzerland

[3] Departamento de Agronomía, Facultad de Ciencias Agrarias, Universidad Nacional de Colombia sede Bogotá, Bogotá, Colombia

[4] Centro de Investigación La Suiza, Corporación Colombiana de Investigación Agropecuaria-Agrosavia,, Km 32 vía al mar, Puerto Arturo, Rionegro, Santander, Colombia

farmers. Colombian cocoa is internationally renowned for its unique flavour and aromatic characteristics, is part of the specialty cocoa group, and occupies the 5th position in global exports (Escobar et al. 2021; FEDECACAO 2022). However, cocoa crops are severely affected by the prevalence of fungal phytopathogens, which cause losses of up to 40% in global and national production (Ten Hoppen et al. 2012; Cabrera et al. 2016).

The most significant diseases affecting Latin America, and the Caribbean are frosty pods and witches' broom, caused by fungi *Moniliophthora roreri* and *M. perniciosa*. These diseases can result in losses of 100 and 90%, respectively (Jaimes and Aranzazu 2010; Marelli et al. 2019; Reyes et al. 2023). Additionally, cocoa productivity can be affected by other diseases such as black pod rot (BPR) caused by the oomycete *Phytophthora* spp., cocoa swollen shoot disease caused by cocoa *swollen shoot virus* (CSSV), and vascular stem dieback (VSD) caused by the basidiomycete *Ceratobasidium theobromae*. Emerging diseases, such as wilt caused by *Ceratocystis* sp. (Mal de machete) and *Rosellinia* spp. (root rot), have increased significantly over the past two decades, destroying large areas of cocoa plantations (Muller and Sackey 2004; Guest and Keane 2007; Kouakou et al. 2012; Cabrera et al. 2016; Rodríguez-Polanco et al. 2020). *Ceratocystis* wilt disease is re-emerging worldwide, particularly in tropical and subtropical regions where cocoa is grown. This disease poses a significant threat to cocoa-producing countries owing to its widespread distribution and rapid spread, identifying it as a high-priority fungal pathogen on a global scale (Cabrera et al. 2016; Lloren 2023).

Ceratocystis wilt is a necrotic vascular disease that affects cocoa plants by damaging the xylem and causing tree death. The incidence of *Ceratocystis* wilt closely relates to transmission modes that naturally occur through the insect *Xyleborus ferrugineus*, recognized as the disease vector (Engelbrecht 2004; Firmino 2011; Santos et al. 2011; Paladines-Rezabala et al. 2022). This insect likely perceives semiochemical signals from the tree, attracting it and facilitating hosting, reproduction, and pathogen spread to healthy trees (Paladines-Rezabala et al. 2022). Additionally, improper human practices, such as using contaminated tools during pruning or pod harvesting, can also transmit this disease (Ferreira et al. 2010; Cabrera et al. 2016). The early identification of *Ceratocystis* wilt symptoms poses a significant challenge, as only advanced stages of this disease are visually detectable, thereby impeding effective control efforts (Tumura et al. 2012; Magalhães et al. 2016; Paladines-Rezabala et al. 2022). The *Ceratocystis* genus comprises approximately 42 species and is divided into four geographical clades: the Latin American clade (LAC), the Asian-Australian clade (AAC), the North American clade (NAC), and the Central African clade (AFC). These clades were established based on phylogenetic analyses using multi-locus (MLST) and combined dataset from several genes (Liu et al. 2018; Marincowitz et al. 2020). However, classifying *Ceratocystis* species is challenging due to the molecular and morphological variability observed within the genus. Many of these species are believed to remain undiscovered, underestimating the diversity of this genus (Ferreira et al. 2010; Oliveira et al. 2015b; Holland et al. 2019). The causal agent of *Ceratocystis* wilt has been associated with different species within the *Ceratocystis* genus as part of a fungal complex termed the *Ceratocystis fimbriata* complex, represented by a group of cryptic species, often classified as an independent species (Marin and Wingfield 2006; Ferreira et al. 2010; Valdetaro et al. 2015; Cabrera et al. 2016).

C. fimbriata complex includes important plant pathogens with variations in geographic origin and host specialization (Engelbrecht and Harrington 2005; de Beer et al. 2014). Over the past decade, there has been a significant increase in the number of studies describing other *Ceratocystis* species within this complex. This can be attributed to the enhanced discriminatory power and precision of molecular information in phylogenetic inference complemented by traditional morphological characterization methods. Together, these approaches contribute to the comprehensive characterization and effective management of the disease (Wyk et al. 2011). In Colombia, *C. fimbriata* Ellis & Halst. 1890, is considered the causal species of *Ceratocystis* wilt disease (Mal de machete) (Arbeláez-Giraldo 1957; ICA 2012). However, there are still inconsistencies among authors that contradict the causal relationship between this pathogen and the disease. Studies comparing DNA sequences have identified new taxa distinct from this species (Marin et al. 2003; Rodas et al. 2008; Van Wyk et al. 2010). For example, Engelbrecht and Harrington (2005) identified *C. cacaofunesta* as a new species within the *C. fimbriata* complex that has been identified as the causal agent for the wilt and death of cacao trees. Therefore, there is a need to correctly identify pathogens in cocoa-producing areas in the country.

This study aimed to clarify and confirm the causal agent responsible for *Ceratocystis* wilt disease (Mal del machete) in cocoa crops in Colombia. To achieve this goal, we characterized isolates of *Ceratocystis* spp. collected from cocoa-producing areas in Colombia at both morphological and molecular levels. The morphological features and molecular information generated in this study will significantly contribute to the accurate and timely diagnosis of this disease.

Materials and methods

Sampling and isolations

The *Ceratocystis* spp. isolates were obtained from symptomatic cacao plants found in four departments of Colombia (Table 1). The strains were collected in 2020, under AGROSAVIA framework collection permit No.1466 from 2014, updated by the 04039 resolution on July 19, 2018. Fungal propagules were obtained from stems and sawdust. The sawdust, found in the surrounding soil, was released by the vector *Xyleborus ferrugineus*. The preparation of woody samples involved cutting the logs into smaller pieces to expose the cambium, using an electric tool previously disinfected with 70% ethanol. For sawdust samples, 50 g of fresh sawdust and soil mixture were collected and placed in labeled paper bags, which were then transported to the laboratory for processing. *Ceratocystis* spp. was isolated following the methodology described by Comissão Executiva do Plano da Lavoura Cacaueira (CEPLAC). This process involves washing the wood chunks with detergent and distilled water and disinfecting them with 70% ethanol and 5% sodium hypochlorite (NaClO) for 2 min, two rinses with distilled water, and a drying process using paper towels. Clean stem pieces and 1 g of the soil and sawdust mixture were placed inside a sandwich-type trap (Barnes et al. 2018) made from treated cocoa pods. The traps were incubated in a humid chamber in darkness at 24 ± 2 °C for 10 days until characteristic structures of the fungus, such as perithecia and ascospores, were detected (Firmino 2011). The masses of ascospores were then removed and placed on Petri dishes containing potato dextrose agar (PDA; OXOID), followed by incubation at approximately 24 ± 2 °C for 10 days until the colonies were obtained. Finally, isolates were preserved on filter paper at room temperature and in agar slant at 4 °C. All isolates were subcultured to ensure a backup culture for subsequent experiments. To differentiate *Ceratocystis* isolates between others genus related to *Ophiostoma* and *Ceratocystopsis*, a cycloheximide sensitivity test was used according to Harrington (1981).

Morphological characteristics of the isolates

Morphologic colony characterization

Monosporic cultures of the selected isolates were conducted following the protocol described by Rodas et al. (2008), with modifications. Sporulated colonies were gently scraped from 10-day-old growth cultures on 2% MEA agar using a soft bristle brush. The scraped spores were homogenized with a sterile solution (5 mL) of distilled water and 1% tween-20, and subsequently agitated for 3 min. Then, 100 µL of the suspension was transferred onto a 2% MEA plates incubating at 24 ± 2 °C for 18 h. Single ascospores were placed in a new Petri dish with 2% MEA.

The morphology of the colonies was assessed according to the growth pattern on the PDA and 2% MEA media after 14 days of incubation at 24 ± 2 °C (Rodas et al. 2008; Firmino 2011). The mycelial growth rate was measured by determining the perpendicular diameter of the colonies every three days over a 14 days incubation period (Firmino 2011). Four replicates were performed for each culture

Table 1 Origin of the isolates of *Ceratocystis* spp. obtained from cocoa producing regions in Colombia, used in this study

ID	Department in Colombia	Municipality	Origin	Map coordinates	
NCF01	Tolima	Rioblanco	Cambium	03°39×26.0”	75°35×45.4”
NCF05	Huila	Gigante	Cambium	NA	NA
NCF07	Santander	Playón	Cambium	07°37’0.53”	73°17’7.62”
NCF10	Valle del Cauca	Palmira	Cambium	03°30’45.9”	76°19’36.6”
NCF15	Huila	Gigante	Cambium	02°24’02.7”	75°31’29.8”
NCF16	Huila	Rivera	Sawdust	NA	NA
NCF17	Huila	Rivera	Sawdust	02°45’19.9”	75°15’35.9”
NCF23	Tolima	Chaparral	Sawdust	03°40×0.09”	75°35×45.4”
NCF24	Tolima	Chaparral	Sawdust	03°40×0.09”	75°35×45.4”
NCF26	Tolima	Falan	Sawdust	05°6×57.5”	74°58×40.2”
NCF27	Tolima	Falan	Sawdust	05°7×24.2”	74°58×30”
NCF28	Tolima	Falan	Sawdust	05°7×24.2”	74°58×30”
NCF29	Tolima	Falan	Sawdust	05°8×27.2”	74°57×37”
NCF30	Tolima	Falan	Cambium	05°8×27.2”	74°57×37”
NCF35	Tolima	Falan	Sawdust	05°8×18.5”	74°58×10.7”
NCF36	Tolima	Falan	Cambium	05°8×18.5”	74°58×10.7”
NCF42	Tolima	Palocabildo	Sawdust	05°7×34.3”	74°59×49.1”
NCF45	Tolima	Palocabildo	Cambium	NA	NA
NCF47	Tolima	Palocabildo	Sawdust	05°7×46.46”	74°59×59.9”

NA not available

medium. Colony color was assessed on the last day of incubation using the Pantone® color palettes (Table S1). The production and distribution of perithecia and ascospores were determined based on four parameters: central group, middle group, entire colony surface, and formation of concentric rings, as described by Marin et al. (2003).

Microscopic isolates characterization

Ceratocystis isolates were grown on 2% malt extract agar (MEA) and maintained at 24 ± 2 °C for a period of 14 days. Fungal structures were collected from each dish using 5 mL distilled water, after which 30 µL of the collected material was placed on a sterile slide and observed under a microscope for visualization (Marin and Wingfield 2006; Firmino 2011; Jabeen and Asad 2017). Morphological characterization included measurement of the perithecial base diameter, neck length, and diameter of ascospores, hyaline endoconidia, and chlamydospores. For each isolate, 50 randomly selected measurements were obtained for each structure. (Marin et al. 2003; Van Wyk et al. 2010; Valdetaro et al. 2015; Liu et al. 2018). Observations also involved the description of the shape of the ostiolar hyphae and conidiophores (Holland et al. 2019). All observations were performed using a light microscope (Carl Zeiss Primo Star, Heidenheim, Germany) coupled with a digital camera (Zeiss Axio CamERc5s) and Zen Blue 3.4 software, with magnification of 10X, 20X and 40X.

Statistical analysis

In the morphological study, the daily growth data of *Ceratocystis* isolates in the culture media were fitted to a mixed linear model using the R package nlme v. 3.1–155 (Pinheiro et al. 2022). The study followed a completely randomized design with isolation, culture medium as fixed effects, and repetition as a random factor. The Fisher LSD test (least significant difference) was performed at a 5% significance level using R v. 4.1.3. (R Core Team 2022). The relationship between the growth of the isolates in the two-culture media was modeled using simple linear regressions, with the slope identified as the average growth rate. Microscopic measurement records were used to determine the mean (mean), standard deviation (SD), maximum (max), and minimum (min) of the evaluated structure width and length for each isolate. Measurements are presented as [(min−) (mean − SD) − (mean + SD) (−max)] (Rodas et al. 2008; Van Wyk et al. 2010; Oliveira et al. 2015a; Liu et al. 2018).

Principal Component Analysis was applied to examine the inter-relationship between the isolates of *Ceratocystis* and the morphological traits that significantly contributed to the variation (Jollife and Cadima 2016). The analysis was conducted using the statistical software R v. 4.1.3, employing the FactoMineR and Factoextra packages (Lê et al. 2008; Kassambara and Mundt 2020). The correlation coefficient (r) was based on the Pearson's correlation between a variable and its principal component (Abdi and Williams 2010).

A conglomerate grouping methodology was used to categorize the 19 tested isolates of *Ceratocystis* spp. This method grouped individuals based on their similarity, using morphological and microscopic characteristics, origin region, and the originating tissue or substrate (Ward 1963; Mota-Gutierrez et al. 2018). Each cluster was described according to the average values of the morphological and microscopic features observed. The analysis was performed using R software version 4.1.3, with the FactoMineR package and the HCPC (Hierarchical Clustering on Principal Components) function.

Molecular characterization of isolates

DNA extraction

DNA was extracted from the morphologically characterized monosporic isolates. To get started, four discs (5 mm) of growing mycelia were inoculated into 250 mL of malt extract broth and incubated at 24 ± 2 °C under shaking conditions for 7 days (de Beer et al. 2014; Suwandi et al. 2021). The resulting mycelia were filtered using miracloth (Merck Millipore) and dried overnight. Subsequently, dry mycelia were collected in 50 mL Falcon tubes for DNA extraction. Dry mycelium lysis was achieved by macerating in a sterile mortar with liquid nitrogen until pulverization. DNA extraction was performed using CTAB Buffer (Griffith and Shaw 1998) following the standardized method established in the Laboratory of Sustainable Perennial Crops of the Agricultural Research Service (ARS) USDA (US Department of Agriculture). The DNA concentrations were measured using an ND-2000 spectrophotometer (NanoDrop® Thermo Scientific). Working stock solutions were prepared by diluting DNA samples with TE buffer to a final concentration of 50 ng/µL.

PCR and sequencing

Molecular characterization of *Ceratocystis* isolates was carried out using the nucleotide sequences of four gene regions, including the β-tubulin gene (*βT-1*), guanine nucleotide-binding protein (*MS204*), second largest subunit of RNA polymerase II (*RPBII*), and 60 S ribosomal protein L37 gene (*FG1093*) (Suwandi et al. 2021; Liu et al. 2018; Fourie et al. 2014). The primer sequences used for the amplification of the four loci are summarized in Table 2. PCR

reactions were conducted in a 25 µL volume containing 1 U Taq DNA polymerase, 0.2 mM dNTPs, 1.5 mM $MgCl_2$, 1X Buffer, 0.5 µM of each primer, and 2 µL of DNA (50 ng/µL) and were run in a Biorad T100 thermocycler. Loci amplification included an initial denaturation step at 94 °C for 2 min, followed by 35 cycles of 30 s at 94 °C, 30 s at 57 °C for gene region *βT1*, *RPBII*, *MS204*, and 60 °C for gen *FG1093*, extension at 72 °C for 1 min, and final extension phase at 72 °C for 5 min. The PCR products were visualized using 1.5% agarose gel electrophoresis with SYBR Safe (Invitrogen). For locus sequencing, PCR amplicons were purified and sequenced using the Sanger method. The resulting sequences were edited using BioEdit v. 7.2.5.0 (Hall 2004). Sequence analysis was performed by comparison with the National Center for Biotechnology Information database (NCBI) using the Basic Local Alignment Search Tool (BLAST) (Firmino 2011; Liu et al. 2018).

Multi-gene phylogenetic analyses

Phylogenetic analysis of the strains obtained in this study within the genus *Ceratocystis* was performed based on the selected loci. To enhance taxonomic analysis, we included loci sequences published in public databases, including *Ceratocystis* species with publicly available information, including *Ceratocystis albifundus* M.J. Wingf., De Beer & M.J. Morris 1996, *Ceratocystis cacaofunesta* Engelbr. & T.C. Harr. 2005, *Ceratocystis colombiana* M. van Wyk & M.J. Wingf. 2010, *Ceratocystis eucalypticola* M. van Wyk & M.J. Wingf. 2012, *Ceratocystis fimbriata* Ellis & Halst. 1890, *Ceratocystis harringtonii* Z.W. de Beer & M.J. Wingf. 2013, *Ceratocystis lukuohia* I. Barnes, T.C. Harrin. & L.M. Keith 2018, *Ceratocystis manginecans* M. van Wyk, Al-Adawi & M.J. Wingf. 2007, *Ceratocystis platani* (J.M. Walter) Engelbr. & T.C. Harr. 2005, and *Ceratocystis smalleyi* J.A. Johnson & T.C. Harr. 2006. Additionally, we included four loci sequences from *Ceratocystis* sp. with genome assemblies published in the databases. To achieve this, we extracted each locus from the genomic sequences, using *C. fimbriata* Ellis & Halst. 1890 locus sequences as seeds. The location of the loci in the genomes was determined by aligning the seed to every genome using BLASTn v. 2.2.3 and extracting them with getfasta tool from the BEDTools suite v. 2.30.0 (Quinlan 2014).

Table 2 Primers utilized for amplification and sequencing of *Ceratocystis* spp. isolates from cacao crops

Gen	Primer	Primer sequence (5′–3′)	Reference
FG1093	FG1093.ceratoF FG1093.ceratoR	GCG CCA CAA CAA GTC GCA CGT TTC TCC GCT TGC CCT TGT CRS	Fourie et al. (2014)
MS204	MS204F.ceratoB MS204R.ceratoB	GGC TGA GCA GCT GAT CCT T ATG TCC GGG TAG TGT TAC CG	Liu et al. (2018) and Fourie et al. (2014)
RPBII	RPB2 5Fb RPB2 7Rb	GAY GAY CGT GAT CAC TTY GG CCC ATR GCY TGY TTR CCC AT	Liu et al. (2018)
βT-1	βt1a βt1b	TTCCCCCGTCTCCA CTTCTTCATG GACGAGATCGTTCA TGTTGAACTC	Liu et al. (2018) and Glass and Donaldson (1995)

The consensus sequences were aligned using the 'auto' alignment option in MAFFT v. 7.515 (Katoh et al. 2018). Poorly aligned regions were identified and removed using TrimAl v. 1.4.1 (Capella-Gutiérrez et al. 2009), and Jalview Software v. 2.11.2.6 (Procter et al. 2021). We conducted a phylogenetic analysis using IQTree v. 2.2.0.3 (Quang-Minh et al. 2022), utilizing a partition matrix created with FASconCAT-G v. 1.05.1 (Kück and Longo 2014). Maximum likelihood (ML) and Bayesian inference (BI) were applied to the combined datasets of the four genes for tree construction. ML analyses were conducted with IQTree v. 2.2.0.3 (Quang-Minh et al. 2022), and the most appropriate models for each locus were as follows: *βT-1*: K2P + R2, *FG1093*: HKY + F + G4, *MS204*: K2P + G4, and *RPBII*: TNe + I. 1000 bootstrap replicates with Shimodaira-Hasegawa-like Approximate Likelihood Ratio Test (SH-aLRT) and Ultra-fast Bootstrap (UFBoot) were used to determine node confidence levels. *Ceratocystis pirilliformis* I. Barnes & M.J. Wingf. 2003, was chosen as the outgroup to root trees. Bayesian analyses were performed using the Markov Chain Monte Carlo (MCMC) algorithm implemented in the MrBayes v. 3.2.7 program (Ronquist et al. 2020), which lasted until the average standard deviation of the split frequencies was < 0.01 and the model of nucleotide substitutions used was GTR + G + I. The tree search involved four separate chains for 1.000.000 generations, with tree sampling occurring every 100th tree. Additionally, the first 25% of trees were discarded. The consensus tree was viewed in Figtree v. 1.4.4 (Rambaut 2018).

Results

Isolates and morphologic colony characterization

A collection of 19 isolates of *Ceratocystis* spp. was obtained from different substrates (sawdust and cambium) on a PDA culture medium. In the cycloheximide sensitivity test, no growth was observed in any of the isolates, confirming that the obtained isolates belonged to the genus *Ceratocystis* and not to *Ceratocystopsis* or *Ophiostoma*, which are tolerant to this antibiotic.

The isolates were categorized into three distinct groups according to morphological characteristics, including color, texture, and colony shape, as well as microscopic features, such as the distribution of ascospores and perithecia during colony growth on PDA and 2% MEA medium (Fig. 1). Isolates NCF16 and NCF01, representing group 1, exhibited colony morphology characterized by dense hyaline aerial mycelium, irregular margins, and scattered perithecia with limited presence of ascospores. Group 2 consisted of isolates (NCF05, NCF07, NCF10, NCF15, NCF17, NCF23, NCF24, NCF26, NCF27, NCF28, NCF29, NCF30, NCF35, NCF36, NCF42, and NCF47), displaying a colony with a woolly appearance, limited elevation, and wavy and irregular light-colored edges, accompanied by abundant production of salmon-colored perithecia and ascospores. Group 3 consisted of isolate NCF45, whose colony had a cottony texture on both media with irregular edges and limited production of perithecia and ascospores.

The isolates exhibited colonies with variations in grayish color and light brownish tones (2325 C, 2328 C). Light gray colors (423 C, 424 C, 2332 C, 2333 C) predominated at the edges of the colonies with a woolly texture, and an olive-green coloration (7761 C–5835 C) appeared at the colony periphery due to submerged mycelium in the culture medium. The reverse surface of the colonies showed dark coloration (Black C, 3 C, and 7 C) (Pantone®) (Table S1).

All the isolates emitted distinctive fruity odor characteristics of *Ceratocystis.* The presence of perithecia and ascospores was evident in the colonies in both the culture media. From the sixth day of growth, perithecia were observed on

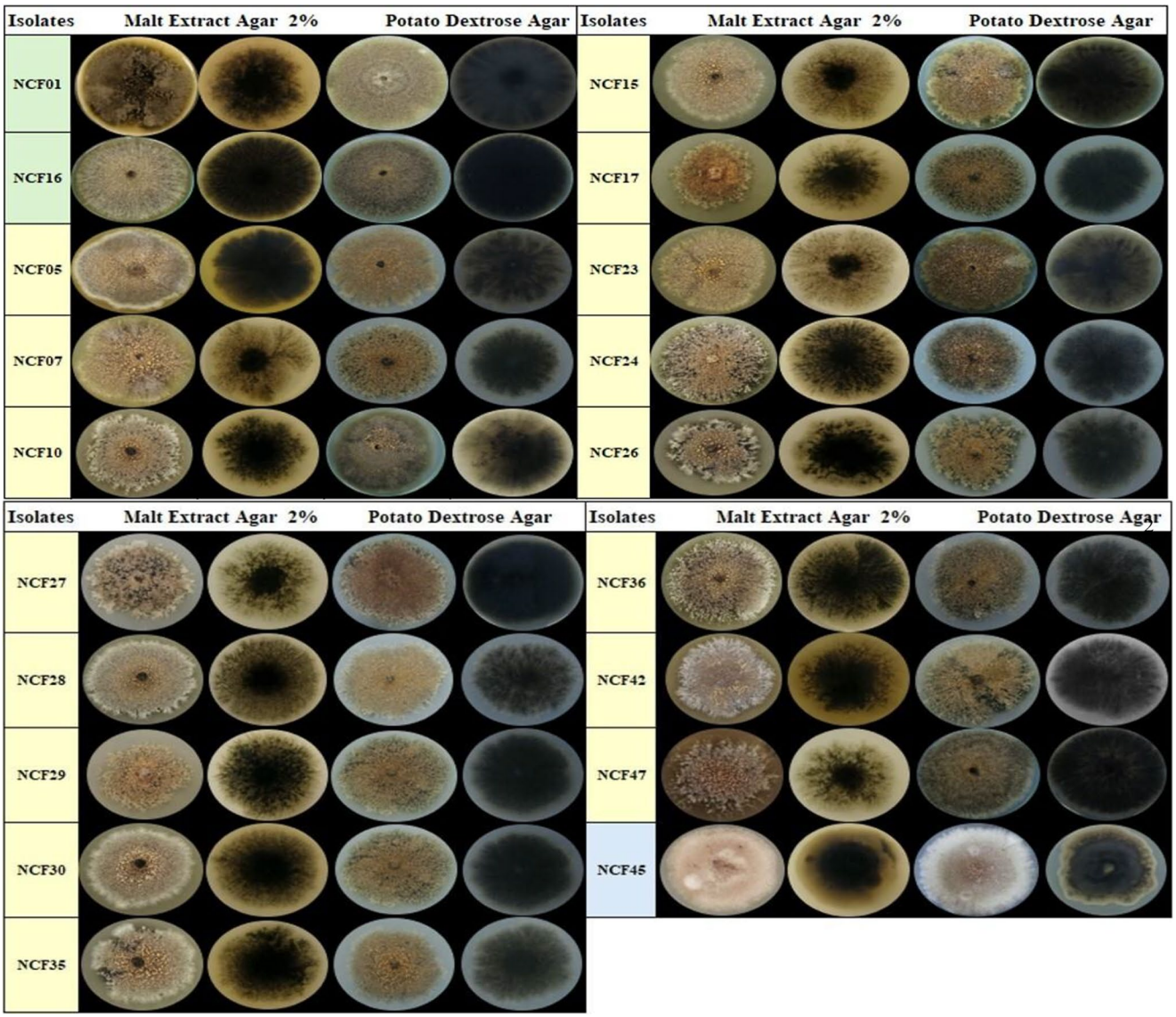

Fig. 1 Growth of isolates in PDA and 2% MEA medium. Pictures were taken after 14 days of incubation at 24 ± 2 °C. *Green*, *yellow*, and *blue-colored* boxes identify isolates belonging to groups 1, group 2, and group 3, respectively, based on morphological characteristics

the surface or submerged in the medium, either individually or in scattered groups. Salmon-colored ascospores were visible in the apical part of the perithecia. The identified distribution pattern of the perithecium was central over the entire surface of the colony, with the latter being the most prominent. Growth data for all isolates were fitted to a polynomial (linear) trend line for both media types, yielding determination coefficients (R^2) of 0.99 for PDA (potato dextrose agar) and 0.99 for 2% MEA (malt extract agar) (Fig. S1). PDA medium consistently supported higher growth across most isolates, with an average growth of 7.26 cm after 14 days and a daily growth rate of 0.53 cm, compared to MEA, which averaged 6.73 cm and had a growth rate of 0.47 cm per day. Among the isolates, NCF47 exhibited the greatest growth on PDA, averaging 8.83 cm, while NCF35 had the lowest growth at 4.96 cm. In MEA, NCF16 showed the highest growth with an average of 8.75 cm, while NCF26 had the lowest at 5.03 cm. No significant differences were observed between isolates NCF01, NCF28, and NCF36 in MEA. Overall, the statistical analysis identified significant differences ($p \leq 0.05$) between isolates and media; however, isolates NCF17, NCF30, NCF24, and NCF42 did not show significant variation (Fig. S2). Based on this analysis, the PDA culture medium was the most favorable for the growth of all the isolates evaluated.

Microscopic characterization of the isolates

At the microscopic level, variations in the dimensions of the analyzed structures were observed within each isolate (Table 3). The isolates produced black perithecia with a globose base, ranging in diameter from 97.0 to 412 × 103–449 µm, surrounded by a dense network of hyphae. The perithecial necks were 120–1020 µm in length and dark in color. At the apical part, ostiolar hyphae were observed, appearing hyaline and divergent, non-septate, straight, or flexuous, which made accurate measurement difficult. In this study, cylindrical endoconidia were exclusively produced in all the isolates, exhibiting different sizes (2.8–7.3 × 9.5–33.4 µm). The endoconidia were produced on a light brown endoconidiophore, septate, with thin walls, and adopting a tubular shape towards the tip. Aleuroconidia were rarely observed in chains, mostly singly, displaying a color range from light to dark brown, a subglobose shape, and smooth wall (6.8–15.0 × 8.0–16.3 µm). Hyaline ascospores were noted in droplets at the tips of the perithecia neck, exhibiting a hat shape and diameters between 3.0 and 6.9 × 3.4–8.2 µm.

The NCF16 isolate was distintive from the rest of the group of *Ceratocystis* isolates. Its perithecia base (117−) 164–237 (−412) × (121−) 192–246 (−449) µm and neck (702−) 766–944 (−1020) µm were the widest and longest, respectively. It also featured the longest endoconidia (3.2−) 4.0–5.2 (−7.3) × (17.3−) 19.5–26.7 (−33.4) µm, and the ostiolar hyphae exhibited a different shape compared to the other isolates. The ostiolar hyphae were longer and more flexible, resembling a long brush, which was not observed in any of the other isolates (Fig. 2).

Principal component analysis (PCA)

The PCA revealed an accumulated variability of 83.1% among the microscopic characteristics of the *Ceratocystis* spp. isolates (Fig. S3). This variability was explained in three dimensions, dimension 1 (45.5%), dimension 2 (22.1%), and dimension 3 (15.5%). Dimension 1 was represented by all the microscopic morphological variables evaluated. The isolates NCF15, NCF23, NCF05, and NCF10 were influenced in this dimension by the size of the bases of the perithecium and ascospores. Isolates NCF16 and NCF30 in dimension 2 were influenced by the length of the perithecium neck and the diameter of the endoconidia. In dimension 3, the isolates NCF01, NCF07, NCF17, NCF24, NCF26, NCF27, NCF28, NCF29, NCF35, NCF36, NCF42, NCF45 and NCF47 were grouped according to the size of the aleuroconidia (Fig. 3). This suggests that there is no single predominant morphological characteristic to identify *Ceratocystis* spp. of cocoa.

Conglomerate analysis categorized the *Ceratocystis* spp. isolates into three clusters, based on the similarity of their morphological microscopic characteristics (Fig. 4). Cluster 1 (21%) comprised isolates identified by the base of the perithecia and the size of the ascospores. It included two isolates from Huila (NCF05 and NCF15), one from Valle del Cauca (NCF10), and one from Tolima (NCF23). Cluster 2 (5.2%) contained only one isolate (NCF16) characterized by the longest perithecia and endoconidia. This isolate was obtained from a sawdust sample collected from the Huila region. Cluster 3 (73.6%), the largest cluster, encompassed 14 isolates, including 12 from Tolima (NCF01, NCF24, NCF26, NCF27, NCF28, NCF29, NCF30, NCF35, NCF36, NCF42, NCF45, and NCF47), one from Santander (NCF07), and one from Huila (NCF17), associated with the size of the aleuroconidia.

Molecular characterization of isolates

DNA extraction and PCR sequencing

DNA extraction was effectively carried out for the 17 isolates evaluated, with concentrations ranging from 236.1 ng/µL to 2771.0 ng/µL. Electrophoresis on a 1.5% agarose gel confirmed the high quality of the extracted DNA with minimal levels of degradation and contamination detected.

Table 3 Range in sizes (micrometers) of microscopic features of isolates of *Ceratocystis* spp. from four departments of Colombia (Huila, Tolima, Valle De Cauca, and Santander)

Isolate	Perithecia (µm)		Endoconidia (µm)	Aleuroconidia (µm)	Ascospores (µm)
	Base (diameter)	Neck (length)			
NCF01	(97−) 125–207 (−274) [a] × (103−) 129–239 (−407) [b]	(288−) 376–555 (−792)	(3.0−) 3.8–4.7 (−5.8) × (9.5−) 16.2–20.4 (−24.5)	(8.3−) 9.6–11.1 (−11.9) × (10.2−) 11.4–13.6 (−13.9)	(3.7−) 3.8–4.8 (−6.2) × (4.4−) 5.1–6.3 (−6.8)
NCF05	(120−) 179–248 (−257) × (143−) 205–260 (−276)	(305−) 393–506 (−523)	(3.1−) 3.7–4.8 (−5.8) × (12.2−) 15.5–17.4 (−18.9)	(8.2−) 9.2–10.3 (−10.9) × (9.1−) 10.1–12.2 (−13.0)	(4.0−) 4.9–5.9 (−6.0) × (5.1−) 6.2–7.4 (−7.9)
NCF07	(167−) 174–210 (−232) × (184−) 199–247 (−291)	(356−) 407–494 (−536)	(3.0−) 3.8–4.8 (−5.9) × (16.0−) 18.5–21.6 (−23.8)	(8.1−) 8.9×10.2 (−10.8) × (10.0−) 11.7–13.4 (−13.9)	(4.0−) 5.0–5.9 (−6.0) × (5.1−) 6.1–7.6 (−7.9)
NCF10	(128−) 191–291 (−364) × (148−) 208–305 (−375)	(247−) 386–538 (−567)	(3.6−) 4.0–5.2 (−7.3) × (16.1−) 19.9–24.4 (−28.0)	(6.8−) 8.5–11.2 (−13.0) × (8.9−) 11.0–13.9 (−16.2)	(4.2−) 4.7–6.2 (−6.9) × (3.8−) 4.7–6.7 (−7.5)
NCF15	(157−) 194–263 (−347) × (193−) 222–289 (−344)	(323−) 381–532 (−592)	(3.5−) 3.8–5.0 (−6.1) × (15.1−) 18.7–24.0 (−27.7)	(8.2−) 9.2–11.6 (−13.0) × (8.3−) 9.9–12.7 (−14.8)	(4.1−) 4.7–6.0 (−6.7) × (5.1−) 5.6–6.9 (−7.9)
NCF16	(117−) 164–237 (−412) × (121−) 192–246 (−449)	(702−) 766–944 (−1020)	(3.2−) 4.0–5.2 (−7.3) × (17.3−) 19.5–26.7 (−33.4)	(7.2−) 8.5–10.0 (−11.8) × (8.0−) 11.3–13.4 (−14.9)	(3.7−) 3.9–5.1 (−5.8) × (4.2−) 4.9–5.9 (−6.5)
NCF17	(131−) 160–239 (−324) × (152−) 167–248 (−332)	(120−) 272–462 (−553)	(3.0−) 3.6–5.1 (−6.0) × (13.4−) 15.3–21.5 (−26.7)	(7.4−) 9.5–11.8 (−14.3) × (9.3−) 11.3–14.0 (−15.6)	(3.8−) 4.4–5.7 (−6.0) × (4.6−) 5.6–6.7 (−8.2)
NCF23	(121−) 182–252 (−268) × (171−) 200–267 (−318)	(354−) 403–498 (−548)	(3.3−) 4.0–5.1 (−5.9) × (16.2−) 18.1–22.7 (−25.3)	(9.1−) 9.7–11.2 (−12.9) × (10.1−) 10.8–12.6 (−13.8)	(4.0−) 4.9–5.7 (−6.4) × (4.3−) 5.8–6.9 (−7.4)
NCF24	(128−) 172–229 (−262) × (141−) 193–243 (−297)	(209−) 294–405 (−431)	(3.2−) 3.6–5.0 (−6.0) × (12.3−) 15.7–22.7 (−29.2)	(8.7−) 9.7–11.8 (−13.6) × (8.9−) 11.6–13.2 (−14.9)	(3.5−) 4.0–4.9 (−5.3) × (4.4) 5.2–6.4 (−7.5)
NCF26	(128−) 172–229 (−262) × (141−) 193–243 (−297)	(209−) 294–405 (−431)	(3.0−) 3.7–4.9 (−5.5) × (15.1−) 16.7–23.9 (−29.6)	(9.1−) 10.4–12.4 (−13.1) × (10.8−) 12.1–14.2 (−16.1)	(4.0−) 4.2–4.8 (−5.3) × (4.0−) 5.2–6.1 (−6.7)
NCF27	(142−) 165–203 (−223) × (163−) 189–243 (−274)	(244−) 275–360 (−438)	(3.2−) 3.7–4.7 (−4.9) × (11.8−) 14.6–17.9 (−18.9)	(9.0−) 10.8–12.9 (−14.1) × (10.9−) 12.5–14.3 (−14.9)	(3.5−) 4.1–5.1 (−5.5) × (3.6−) 5.1–6.1 (−6.9)
NCF28	(130−) 157–207 (−259) × (148−) 172–218 (−251)	(161−) 225–307 (−376)	(3.2−) 3.7–4.9 (−6.1) × (15.9−) 15.9–22.5 (−26.8)	(9.1−) 10.0–11.5 (−13.4) × (10.8−) 11.3–13.5 (−15.7)	(3.0−) 3.7–5.0 (−5.5) × (4.2−) 5.7–6.6 (−7.0)
NCF29	(107−) 159–211 (−223) × (105−) 177–212 (−240)	(244−) 342–468 (−522)	(2.8−) 3.3–4.7 (−5.8) × (13.7−) 14.4–17.8 (−24.3)	(8.2−) 9.2–10.3 (−10.9) × (10.1−) 12.3–14.4 (−15.1)	(3.8−) 4.2–5.1 (−5.9) × (4.0−) 4.9–5.8 (−6.6)
NCF30	(162−) 200–265 (−310) × (140−) 197–242 (−278)	(301−) 425–556 (−695)	(3.3−) 4.1–5.2 (−5.6) × (16.4−) 19.2–25.4 (−27.6)	(10.0−) 10.0–12.4 (−15.0) × (10.1−) 11.4–13.6 (−14.9)	(4.0−) 4.3–5.0 (−5.5) × (4.6−) 5.1–6.3 (−6.8)
NCF35	(124−) 155–212 (−254) × (143−) 172–222 (−247)	(179−) 273–458 (−498)	(3.2−) 3.7–4.9 (−5.7) × (15.1−) 17.0–22.3 (−27.6)	(9.0−) 9.7–11.5 (−12.7) × (10.5−) 11.2–13.3 (−15.1)	(3.9−) 4.2–4.8 (−5.7) × (3.7−) 5.1–6.1 (−7.0)
NCF36	(145) 187–252 (−292) × (145−) 190–250 (−294)	(325−) 420–550 (−604)	(3.1−) 3.9–4.9 (−5.6) × (12.2−) 17.0–22.7 (−29.1)	(9.6−) 10.1–12.2 (−13.5) × (10.9−) 12.2–14.5 (−15.8)	(4.0−) 4.3–5.1 (−5.9) × (5.1−) 5.6–6.5 (−7.0)
NCF42	(140−) 174–219 (−235) × (149−) 181–228 (−290)	(305−) 356–449 (−528)	(3.4−) 3.9–4.9 (−5.7) × (15.0−) 16.9–22.2 (−24.5)	(8.8−) 9.6–11.4 (−13.8) × (10.8−) 11.2–13.0 (−14.8)	(3.0−) 4.1–5.3 (−6.9) × (4.4−) 5.7–6.8 (−7.0)
NCF45	(130) 156–207 (−235) × (120−) 159–210 (−232)	(300−) 402–572 (−651)	(3.3−) 3.9–5.0 (−5.9) × (15.0−) 17.2–23.0 (−28.0)	(9.1−) 9.8–11.9 (−13.5) × (10.3−) 11.3–13.5 (−14.8)	(3.4−) 4.0–5.0 (−5.7) × (3.4−) 5.1–6.3 (−7.0)
NCF47	(129−) 169–215 (−239) × (141−) 178–233 (−264)	(285−) 351–471 (−546)	(3.3−) 3.8–5.1 (−5.8) × (15.1−) 17.5–22.6 (−26.9)	(9.2−) 9.6–11.5 (−13.3) × (10.2−) 11.3–13.6 (−16.3)	(3.5−) 3.9–4.7 (−5.0) × (4.5−) 4.6–5.8 (−6.5)

Measurements are presented as [(minimum−) (mean − SD) − (mean + SD) (−maximum)]

[a]Width

[b]Length

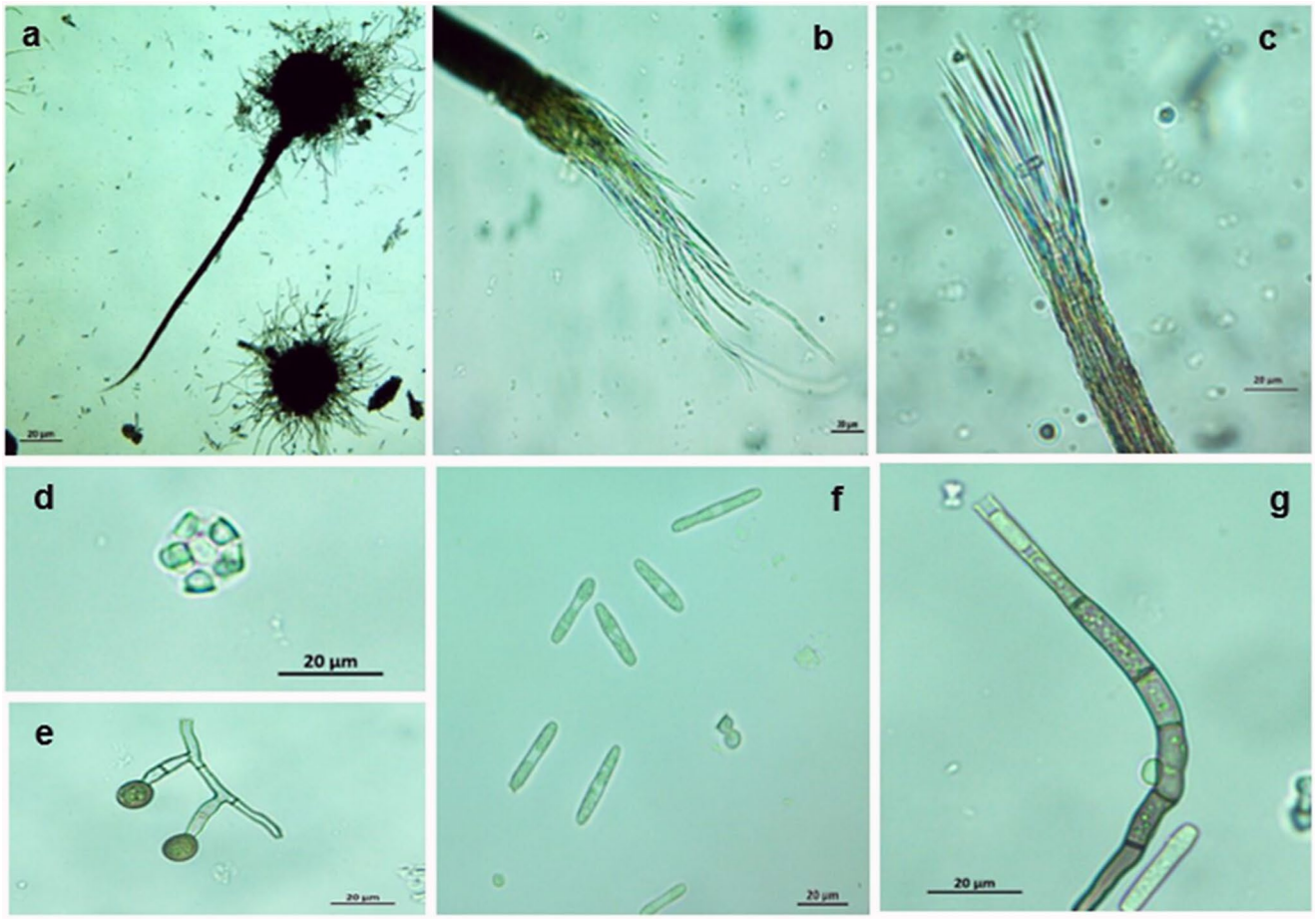

Fig. 2 NCF16 isolation from the Huila Department. Microscopic features observed from 14 days growth on 2% MEA medium at incubation at 24 ± 2 °C. **a** Perithecia with globose base and long neck; **b** elongated brush-shaped ostiolar hyphae; **c** blunt tipped ostiolar hyphae observed in the other isolates evaluated; **d** hat-shaped ascospores; **e** aleuroconidia in solitary; **f** cylindrical endoconidia and **g** endoconidiophore with emerging cylindrical conidia. Scale bars = 20 µm

Amplicons of 600 bp were obtained for *βT-1* and *FG1093*, 1200 bp for *RPBII*, and 970 bp for *MS204* locus. All analyzed sequences were similar to those from *Ceratocystis cacaofunesta* when compared with the information available in GenBank. The similarity values for this species varied from 98.28 to 100% for the *βT-1* gene, from 97.35 to 99.30% for the *MS204* gene, from 99.44 to 100% for the *RPBII* marker, and from 98.01 to 99.61% for the *FG1093*. A few isolates presented high similarity percentages with *C. fimbriata*, *C. papillata*, *C. platani*, *C. acaciivora* and *C. adelpha*, species ranging from 98.97 to 99.67%, respectively (Table S2). This suggests that the identity of the *Ceratocystis* isolates evaluated is most likely *C. cacaofunesta*, based on the BLASTn analysis conducted.

Multi-gene phylogenetic analyses

Compiling the information from the selected markers resulted in a partitioned matrix consisting of 3417 base pairs. The contributions of each marker used in phylogenetic inference were as follows: *βT-1* (632pb), *MS204* (944pb), *FG1093* (635pb), and *RPBII* (1206pb). Phylogenetic inference was conducted using concatenated sequences of the four genomic loci based on the Maximum likelihood (ML) and Bayesian inference (BI) methods, which provided a consistent tree topology (Van Wyk et al. 2010; Fourie et al. 2014). In the phylogenetic tree (Fig. 5), four major clades of *Ceratocystis* species, labeled A, B, C, and D, were strongly supported.

In this study, all collected isolates were most closely grouped in Clade A within the species *C. cacaofunesta.* Clade A was very well supported (99.1% SH-aLRT, 97% UFBoot) Bootstrap (BS) and (1.0) Posterior Probability (PP), and three subgroups were found: the first group contained the isolates NCF16 (Huila-sawdust), NCF36 (Tolima-cambium), and NCF30 (Tolima-cambium). However, branch support was weak (81.1% SH-aLRT, (−) UFBoot) BS and (0.51) PP; the subgroup with isolates NCF17 (Huila-sawdust) and NCF05 (Huila-cambium) had support of (86.8% SH-aLRT, 81% UFBoot) BS and (0.92) PP; the

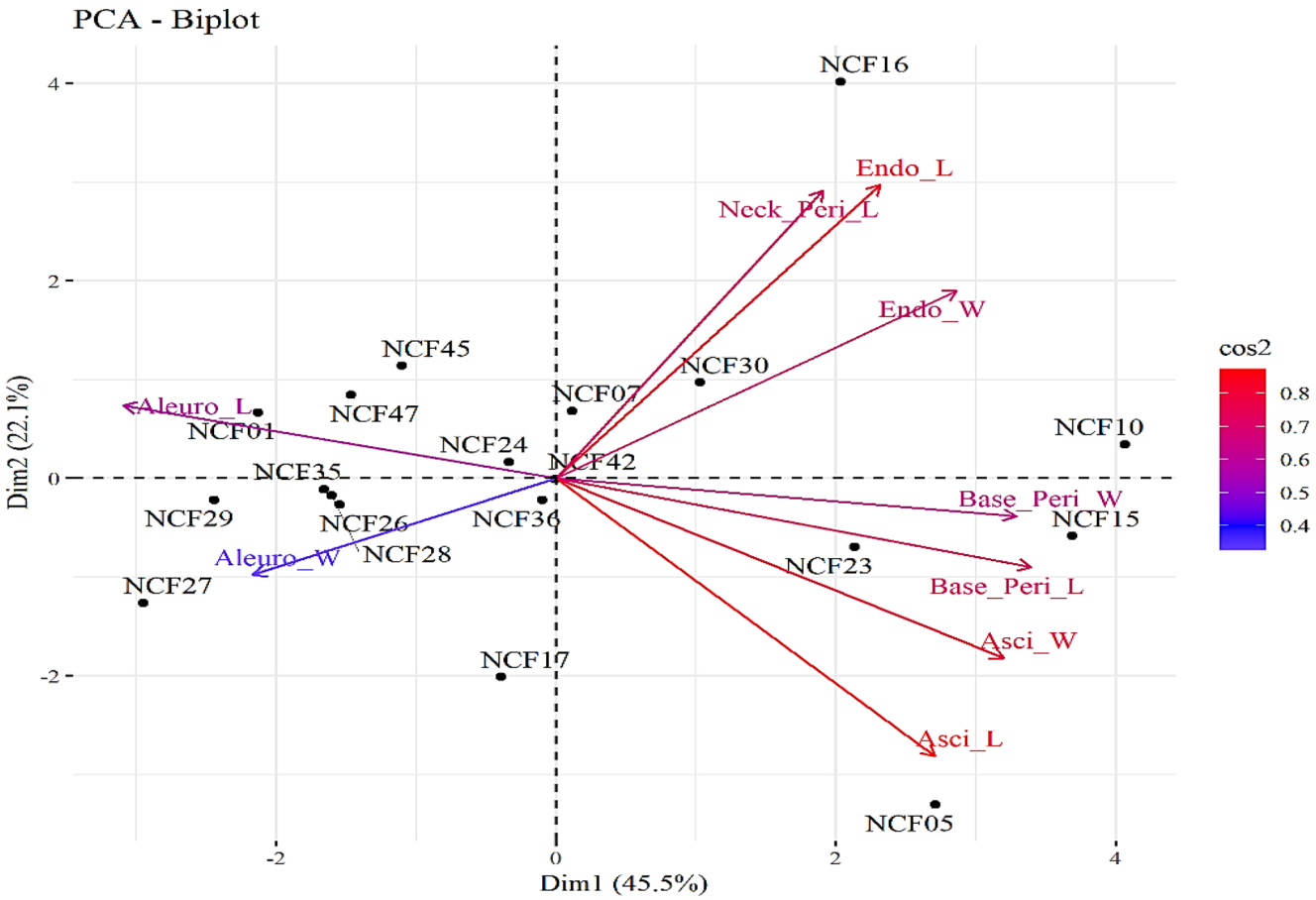

Fig. 3 Biplot for quantitative variables. Principal Component Analysis (PCA). Relationship between microscopic morphological characteristics and isolates of *Ceratocystis* spp. Plots of different morphological variables. Dimension 1, diameter of perithecia, ascospores, endoconidia, and aleuroconidia (NCF05, NCF10, NCF15, and NCF23). Dimension 2, length of perithecia necks and endoconidia (NCF16 and NCF30). Dimension 3, diameter of aleuroconidia (NCF01, NCF07, NCF17, NCF24, NCF26, NCF27, NCF28, NCF29, NCF35, NCF42, NCF45 and NCF47)

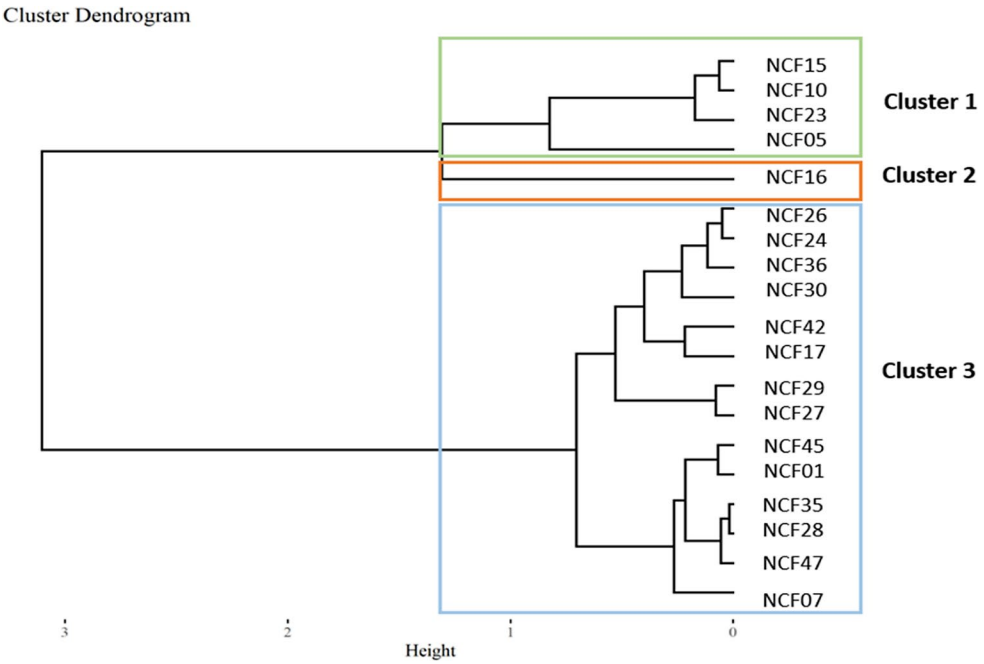

Fig. 4 Cluster dendrogram based on morphological, microscopic characteristics, and the origin of the isolates of *Ceratocystis* spp. evaluated in this study. Cluster 1 (NCF15, NCF10, NCF23, and NCF05); Cluster 2 (NCF16); Cluster 3 (NCF26, NCF24, NCF36, NCF30, NCF42, NCF17, NCF29, NCF27, NCF45, NCF01, NCF35, NCF28, NCF47, and NCF07)

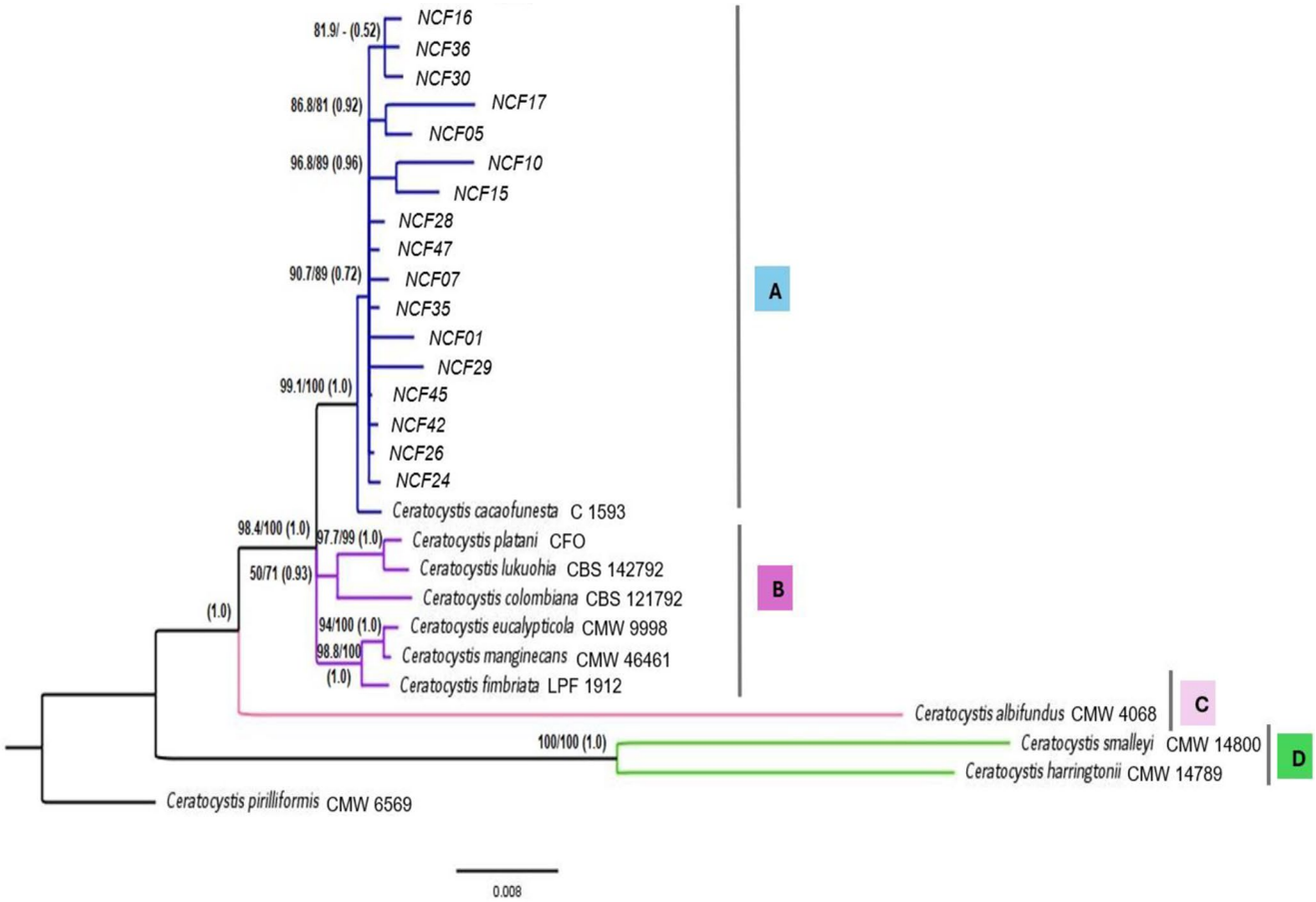

Fig. 5 Consensus phylogenetic tree derived from both Maximum-likelihood and Bayesian Inference methods based on combined sequence data from the *βt-1*, *MS204*, *FG1093*, and *RPBII* genes. It shows relationships between reference *Ceratocystis* species (*C. albifundus*, *C. colombiana*, *C. cacaofunesta*, *C. fimbriata*, *C. platani*, *C. harringtonii*, *C. smalleyi*, *C. pirilliformis*, *C. manginecans*, *C. eucalypticola*, *C. lukuohia*), and *Ceratocystis* isolates (NCF01, NCF05, NCF07, NCF10, NCF15, NCF16, NCF17, NCF24, NCF26, NCF28, NCF29, NCF30, NCF35, NCF36, NCF42, NCF45, and NCF47) obtained from cocoa producing regions in Colombia. Support values (SH-aLRT/UFBoot) Bootstrap and (PP) Posterior Probability are shown above the branches. Bootstrap values < 50% are marked with (–)

subgroup with isolates NCF10 (Valle del Cauca-cambium) and NCF15 (Huila-cambium) had supported of (96.8% SH-aLRT, 89% UFBoot) BS and (0.96) PP. Clade B included the reference species, *C. platani*, *C. lukuohia*, *C. colombiana*, *C. eucalypticola*, *C. manginecans* and *C. fimbriata.* This clade was strongly supported the values (98.4% SH-aLRT, 100% UFBoot) BS and (1.0) PP. The third group (Clade C) corresponded to *C. albifundus*, and the branch nodes were supported by a probability value of (1.0) PP. The Clade D provided support for (100% SH-aLRT, 100% UFBoot) BS, and (1.0) PP for two different species *C. smalleyi*, and *C. harringtonii.*

The combination of the four molecular markers in the phylogenetic analysis successfully distinguished and differentiated eleven species of *Ceratocystis* (*C. albifundus* M.J. Wingf., De Beer & M.J. Morris 1996, *C. colombiana* M. van Wyk & M.J. Wingf. 2010, *C. cacaofunesta* Engelbr. & T.C. Harr. 2005, *C. fimbriata* Ellis & Halst. 1890, *C. platani* (J.M. Walter) Engelbr. & T.C. Harr. 2005, *C. harringtonii* Z.W. de Beer & M.J. Wingf. 2013, *C. smalleyi* J.A. Johnson & T.C. Harr. 2006, *C. pirilliformis* I. Barnes & M.J. Wingf. 2003, *C. manginecans* M. van Wyk, Al-Adawi & M.J. Wingf. 2007, *C. eucalypticola* M. van Wyk & M.J. Wingf. 2012, *C. lukuohia* I. Barnes, T.C. Harrin. & L.M. Keith 2018) used as references in this study.

Discussion

In recent decades, climate change has accelerated the intensification of diseases caused by both known and emerging pathogens in cocoa cultivation, posing significant risks to the global supply and yield of this food. These changes increase outbreak risks by altering pathogen evolution and host-pathogen interactions, which facilitates the emergence and spread of new strains (Cilas and Bastide 2020; Singh et al. 2023). *Ceratocystis* wilt, also known as Machete Wilt, is recognized as a significant emerging disease in Central and

South America and poses a severe threat to cocoa producers globally (Engelbrecht et al. 2007). *Ceratocystis fimbriata* has been reported to be the causative pathogen of machete disease in cocoa in Colombia and has been identified in other crops of interest such as coffee and citrus (Marin and Wingfield 2006; Van WyK et al. 2010). However, the high diversity of this species and the presence of cryptic species in the genus *Ceratocystis* complicate the task of specifically defining the causative agent.

A collection of *Ceratocystis* spp. isolates was established from sawdust and symptomatic tissue samples collected from four departments and nine cocoa-producing municipalities in Colombia. Sawdust samples offered a higher recuperation of isolates in our study, which is particularly significant because conventional isolation methods for such purposes are typically destructive. Holland et al. (2019) and Engelbrecht and Harrington (2005) reported that, in some cases, the primary source of infection can be attributed to soil contamination by aleuroconidia, which are produced by the fungus or released into the soil through sawdust or the excreta of the insect *Xyleborus*. Most species produce these structures to survive in wood or soil (de Beer et al. 2014).

Comparisons of colony morphology revealed colonies with different textures, colors, and forms of distribution and production of perithecia and ascospores. This variability has been previously reported, describing morphological changes associated with growing conditions, such as culture media and temperature (Engelbrecht 2004; Firmino 2011; Oliveira et al. 2015a). In this study, the observed colony growth patterns did not show a unique pattern specific to this cocoa pathogen in Colombia in the evaluated culture medium. Observations indicated that PDA and 2% MEA media provided higher mycelial growth for all isolates tested. These media seem to allow homogeneous growth of the fungus compared to others, making them suitable for the characterization and conservation of *Ceratocystis* at the laboratory level (Santos et al. 2011; Oliveira et al. 2015a). Furthermore, the production of perithecia and ascospores was specific to each isolate regardless of the culture media used. This suggests an isolate-dependent variation in these reproductive structures.

Microscopic characterization of the isolates revealed variations in the morphology and size of certain structures compared to those reported for *C. fimbriata* in different hosts. Differences were observed in aspects related to perithecia and endoconidia. The observed size range for the bases and necks of perithecia was slightly larger than the ranges defined in previous studies (Marin et al. 2003; Oliveira et al. 2015b; Xu et al. 2020), which reported ranges of 80–268 × 110–262 µm and 408–870 µm respectively. In studies related to the morphology of *Ceratocystis*, the shape of the perithecia has been an important feature for taxonomy and classification (Johnson et al. 2005). The observed variations in perithecia size and morphology may indicate potential differences or adaptations within the *Ceratocystis* isolates from this study, which could be of taxonomic interest and contribute to the understanding of the diversity within this fungal genus. Further studies and comparisons with known species or strains may provide valuable insights into the taxonomic significance of these morphological variations.

The endoconidia produced by the isolates in this study were exclusively cylindrical in shape and varied in size, consistent with the description by Firmino (2011), who distinguished 12 types of spores among isolates. The observed dimensions of the cylindrical endoconidia were within the range reported for *C. fimbriata* in cocoa and eucalyptus. Nevertheless, these dimensions differed from those reported by Engelbrecht (2004) and Marin et al. (2003) for this species in coffee crops in Colombia, which were considerably smaller than those observed in our isolates. This suggests the possible presence of a species distinct from *C. fimbriata* in cocoa crops. The absence or presence of doliform conidia in *Ceratocystis* isolates is an important characteristic for identifying species within the *C. fimbriata* complex (Engelbrecht 2004; Van Wyk et al. 2010). In this study, doliform conidia were absent in all the evaluated isolates. Indeed, this is a crucial taxonomic characteristic for identifying *Ceratocystis* isolates from cocoa in Colombia. In contrast, ascospores, aleuroconidia, ostiolar hyphae, and endoconidiophores showed no discernible differences among the isolates. This suggests that while certain morphological characteristics, such as endoconidia shape and size, are consistent with known characteristics of *C. fimbriata*, there may be variations that are relevant for taxonomic identification within the *C. fimbriata* complex.

The NCF16 isolate highlighted in this study showed distinct morphological features compared to other isolates evaluated, such as larger perithecial bases (117−) 164–237 (−412) × (121−) 192–246 (−449) µm and necks, along with endoconidia (3.2−) 4.0–5.2 (−7.3) × (17.3−) 19.5–26.7 (−33.4) µm long, which are consistent with the descriptions of *Ceratocystis cacaofunesta* by Engelbr and Harr (2005). Additionally, this isolate had a unique shape of ostiolar hyphae, resembling a long brush, which was not observed in the other isolates. These findings contribute to the understanding of the morphology of *Ceratocystis* isolates and suggest potential taxonomic implications. Comparisons with known species and molecular analyses would contribute to a more complete understanding of the taxonomic status of NCF16 and its significance in the genus *Ceratocystis*.

Principal Component Analysis (PCA) revealed that microscopic morphological characteristics (perithecia, ascospores, endoconidia, and aleuroconidia) were the most

important variables for discriminating between isolates and grouped them into three main clusters independent of the region and substrate of origin; these findings support the importance of these characteristics in distinguishing fungal taxa (Johnson et al. 2005). Based on the morphological variability found in the *Ceratocystis* spp. isolates from cocoa, it is suggested that macroscopic characteristics alone cannot be used for their identification and characterization at the laboratory level. At the microscopic level, the morphology of the fungus can be influenced not only by natural variation but also by environmental conditions, making species identification based solely on morphological traits potentially confusing (Rodríguez-Polanco et al. 2020; Bejarano et al. 2021). However, considering the emergence of diseases and new pathogens, it is necessary to continue the search for traits that are stable across different species and that facilitate identification and diagnosis, complemented by molecular tools (Valdetaro et al. 2015).

The identification of many *Ceratocystis* species has been associated with sequence data from the *ITS* region. However, the genus *Ceratocystis* presents phylogenetic incongruence and the coexistence of various ITS types within individual isolates, which has cast considerable doubt on delineating species within *Ceratocystis* and the efficacy of using this marker in taxonomic studies (Harrington 2013; Kanzi et al. 2020). Given the degree of similarity between *Ceratocystis* species and their difficult differentiation, the use of conserved gene regions such *βT-1*, *RPBII*, *MS204* and *FG1093*, has been considered as an alternative to support species boundaries within this genus (Fourie et al. 2014). The utilization of appropriate genomic regions in a multigene phylogenetic analysis yields dependable and strong data, enabling the differentiation of various lineages within *C. fimbriata* complex isolates (Fourie et al. 2014; Harrington et al. 2014). According to the above mentioned, in this work, *Ceratocystis* spp. isolates from different Colombian cocoa growing regions, were identified at the genus and species level, such as *C. cacaofunesta* using the combination of sequences from the four molecular markers *βT-1*, *RPBII*, *MS204* and *FG1093*, along with the maximum likelihood (ML) and Bayesian inference (BI) methods. This confirmed the discriminatory power of these markers, which allowed placement of all *Ceratocystis* spp. isolates in the *C. cacaofunesta* cluster, distinguished from the *C. fimbriata* cluster and the *C. fimbriata complex* (s.l.) species. Similar to PCA, phylogenetic analysis did not show grouping of isolates according to their geographical region and substrate of origin.

The findings of this study are congruent with those obtained by Fourie et al. (2014), where the combination of the same molecular markers provided significant support and resolution for the identification of 11 of the 15 species *Ceratocystis* evaluated. Similarly, Liu et al. (2018) identified a new *Ceratocystis* species responsible for black rot symptoms in *Colocasia esculenta* corms in China's YunNan and ShanDong provinces, based on phylogenetic analysis of *ITS*, *BT1*, *TEF-1a*, *MS204*, and *RPBII* regions. The use of these conserved gene regions has also allowed taxonomic classification of *Ceratocystis* species at the clade level. In this study, Colombian cocoa isolates were placed in the Latin American clade (LAC), distinguishing them from species belonging to the Asian-Australian clade (AAC), North American clade (NAC), and Central African clade (AFC). Other studies have reported the use of these markers for the clade-level classification of *Ceratocystis* isolates from diverse hosts and geographical regions (de Beer et al. 2014; Fourie et al. 2014; Barnes et al. 2018; Liu et al. 2018). Additional phylogenetic analysis based on ML and BI, applied to each dataset individually for the *RPBII* and *MS204* markers (data not shown) associated all the *Ceratocystis* spp. cocoa isolates with the species *C. cacaofunesta*, similar to the multilocus analysis. Additionally, it classified, differentiated, and grouped the species within the *C. fimbriata* (s.l.) complex. This demonstrated that *RPBII* and *MS204* could be candidates for use in diagnostic tests for species-level identification of this fungus. According to Fourie et al. (2014), these markers provide more information than other commonly used regions.

According to the characterization of isolates from cocoa plants in Colombia with symptoms of *Ceratocystis* wilt (Mal de machete), the causal agent of this disease is *C. cacaofunesta.* This pathogen exhibited morphological variability at both the macro-and microscopic levels; however, at the molecular level, there were no genetic differences associated with it with other species within the genus. This study is the first to report the identity of the pathogen responsible for this disease in Colombia. This finding represents the first step in studying the epidemiology of the disease, which is present in the main cocoa-producing departments of the country, including Santander, Huila, and Tolima, and in other departments such as the Valle del Cauca, which currently represents a potential region for the crop (MADR 2019). To further characterize the isolates, we recommend conducting pathogenicity tests with Colombian *Ceratocystis* isolates from sawdust and plant tissues on cocoa cultivars according to Koch's postulates. This is essential for establishing host specificity and for generating valuable data to support breeding programs.

Supplementary Information The online version contains supplementary material available at https://doi.org/10.1007/s42161-024-01798-7.

Acknowledgements We are grateful to Corporación Colombiana de Investigación Agropecuaria—AGROSAVIA and Universidad Nacional de Colombia, sede Bogotá, for the financial support of this

research. We acknowledge Dra. Eleonora Rodríguez Polanco for her guidance in understanding the disease and the pathogen.

Author contributions These authors all contributed equally to this work. Authors are listed in alphabetical order by last name.

Funding Open Access funding provided by Colombia Consortium. This work was supported by the Ministerio de Ciencia, Tecnología e Innovación, under Grant 890–2020, Project ID: 82070; and within the framework of the USDA-FAS-Agrosavia agreement, F2 Programa de Manejo Integrado para-Cacao, Project ID: 1000978. CONV_1939 and Universidad Nacional de Colombia sede Bogotá, Project ID: 56120 Código QUIPU: 202010037645 Convocatoria para la financiación parcial de proyectos de tesis de doctorado y maestría de la facultad de ciencias agrarias, sede Bogotá. Fondo de Investigación UGI– 2022.

Declarations

Competing interests The authors declare that they have no conflict of interest.

References

Abdi H, Williams LJ (2010) Principal component analysis. Wiley Interdisciplinary Reviews: Comput Stat 2(4):433–459. https://doi.org/10.1002/wics.101

Arbeláez-Giraldo E (1957) La Llaga macana del tronco del cacao. Palmira: Acta Agro 7(1):71–103. https://revistas.unal.edu.co/index.php/acta_agronomica/article/view/49070 Accessed 28 May 2022

Barnes I, Fourie A, Wingfield MJ, Harrington TC, McNew DL, Sugiyama LS, Luiz BC, Heller WP, Keith LM (2018) New *Ceratocystis* species associated with rapid death of metrosideros polymorpha in Hawaii. Pers: Mol Phylogeny Evol Fungi 40:154–181. https://doi.org/10.3767/persoonia.2018.40.07

Bejarano CAP, Kafuri LA, García JMP (2021) Identification of *Phytophthora* spp. isolates obtained from cocoa crops in Antioquia. Colombia Acta Agro 70(1). https://doi.org/10.15446/acag.v70n1.70619

BLAST® Command Line Applications User Manual. https://scicomp.ethz.ch/public/manual/BLAST/BLAST.pdf. Accessed 10 Sep 2022

Cabrera OG, Molano EP, José J, Álvarez JC, Pereira GA (2016) Ceratocystis Wilt Pathogens: History and Biology—Highlighting C. cacaofunesta, the Causal Agent of Wilt Disease of Cacao. In: Bailey B, Meinhardt L (eds) Cacao diseases. Springer, Cham. https://doi.org/10.1007/978-3-319-24789-2_12

Capella-Gutiérrez S, Silla-Martínez JM, Gabaldón T (2009) TrimAl: a tool for automated alignment trimming in large-scale phylogenetic analyses. Bioinform 25(15):1972–1973. https://doi.org/10.1093/bioinformatics/btp348

Cilas C, Bastide P (2020) Challenges to Cocoa Production in the Face of Climate Change and the spread of pests and diseases. Agronomy 10(9):1232. https://doi.org/10.3390/agronomy10091232

R Core Team (2022) R: a Language and Environment for Statistical Computing. R Foundation for Statistical Computing, Vienna, Austria. Version 4.1.3. https://www.R-project.org/. Accessed 12 May 2022

de Beer ZW, Duong TA, Barnes I, Wingfield BD, Wingfield MJ (2014) Redefining *Ceratocystis* and allied genera. Stud Mycol 79(1):187–219. https://doi.org/10.1016/j.simyco.2014.10.001

Diaz-Valderrama JR, Leiva-Espinoza ST, Aime MC (2020) The history of cacao and its diseases in the Americas. Phytopathology 110:1604–1619. https://doi.org/10.1094/PHYTO-12-18-0477-RVW

Engelbrecht CJB (2004) Host specialization, intersterility, and taxonomy of populations of Ceratocystis fimbriata from sweet potato, sycamore, and cacao. Dissertation, Iowa State University

Engelbrecht CJB, Harrington TC (2005) Intersterility, morphology and taxonomy of *Ceratocystis fimbriata* on sweet potato, cacao, and sycamore. Mycologia 97(1):57–69. https://doi.org/10.3852/mycologia.97.1.57

Engelbrecht CJ, Harrington TC, Alfenas A (2007) *Ceratocystis* wilt of cacao - A disease of increasing importance. Phytopathology 97(12):1648–1649. https://doi.org/10.1094/PHYTO-97-12-1648

Escobar S, Santander M, Zuluaga M, Chacon I, Rodríguez J, Vaillant F (2021) Fine cocoa beans production: tracking aroma precursors through a comprehensive analysis of flavour attributes formation. Food Chem 365:130627. https://doi.org/10.1016/j.foodchem.2021.130627

FEDECACAO (2022) Año cacaotero 2020–2021, el de mayor producción de cacao en la historia de Colombia. https://www.fedecacao.com.co/post/a%C3%B1o-cacaotero-2020-2021-el-de-mayor-producci%C3%B3n-de-cacao-en-la-historia-de-colombia. Accessed 8 May 2023

Ferreira EM, Harrington TC, Thorpe DJ, Alfenas AC (2010) Genetic diversity and interfertility among highly differentiated populations of *Ceratocystis fimbriata* in Brazil. Plant Pathol 59(4):721–735. https://doi.org/10.1111/j.1365-3059.2010.02275.x

Firmino AC (2011) Caracterização de isolados de *Ceratocystis* sp., avaliação de resistência clonal de eucalipto e sensibilidade deste fungo a diferentes fungicidas. Dissertation, Universidade Estadual Paulista

FONTAGRO (2020) La Cadena de Valor del Cacao en América Latina y El Caribe. https://www.fontagro.org/new/uploads/adjuntos/Informe_CACAO_linea_base.pdf. Accessed 22 May 2023

Fourie A, Wingfield MJ, Wingfield BD, Barnes I (2014) Molecular markers delimit cryptic species in *Ceratocystis* Sensu Stricto. Mycol Prog 11:1020. https://doi.org/10.1007/s11557-014-1020-0

Glass NL and Donaldson GC (1995). Development of primer sets designed for use with the PCR to amplify conserved genes from filamentous Ascomycetes. Appl Environ Microbiol. 61(4): 1323–1330. https://doi.org/10.1128/aem.61.4.1323-1330.1995

Griffith GW, Shaw DS (1998) Polymorphisms in *Phytophthora infestans*: four mitochondrial haplotypes are detected after PCR amplification of DNA from pure cultures or from host lesions. Appl Environ Microbiol 64(10):4007–4014. https://doi.org/10.1128/aem.64.10.4007-4014.1998

Guest D, Keane P (2007) Vascular-streak dieback: a new encounter disease of cacao in Papua New Guinea and Southeast Asia caused by the obligate basidiomycete *Oncobasidium theobromae*. Phytopathology 97:1654–1657. https://doi.org/10.1094/PHYTO-97-12-1654

Hall T (2004) BioEdit Versión 7.0.0. Manual. https://studylib.net/doc/14572292/bioedit-version-7.0.0. Accessed 5 Oct 2022

Harrington TC (1981) Cycloheximide sensitivity as a taxonomic character in *Ceratocystis*. Mycologia 73(6). https://doi.org/10.2307/3759682

Harrington TC (2013) Ceratocystis Diseases. Chapter 11. Iowa (US): P. Gonthier & G. Nicolotti. https://faculty.sites.iastate.edu/tcharrin/files/inline-files/CeratocystisDiseases2013_1.pdf. Accessed 18 May 2023

Harrington TC, Kazmin MR, Al-Sadi AM, Ismail SI (2014) Intraspecific and intragenomic variability of ITS rDNA sequences reveals taxonomic problems in *Ceratocystis fimbriata* sensu stricto. Mycologia 106(2):224–242. https://doi.org/10.3852/13-189

Holland LA, Lawrence DP, Nouri MT, Travadon R, Harrington TC, Trouillas FP (2019) Taxonomic revision and multi-locus phylogeny of the north American clade of *Ceratocystis*. Fung Syst Evol 3:135–156. https://doi.org/10.3114/fuse.2019.03.07

ICA (2012) Manejo fitosanitario del cultivo del cacao. Medidas para la temporada invernal. https://www.ica.gov.co/getattachment/c01fa43b-cf48-497a-aa7f-51e6da3f7e96/-. Accessed 21 Jun 2022

Jabeen K, Asad S (2017) Assessment of selected culture media for competent growth characteristics of Ceratocystis manginecans (cause of Mango Sudden Death). J Bio Env Sci 148(5):148–154. https://www.researchgate.net/publication/330505610_Assessment_of_selected_culture_media_for_competent_growth_characteristics_of_Ceratocystis_manginecans_Cause_of_Mango_Sudden_Death/link/606ef7f092851c8a7bb0ace9/download?_tp=eyJjb250ZXh0Ijp7ImZpcnN0UGFnZSI6InB1YmxpY2F0aW9uIiwicGFnZSI6InB1YmxpY2F0aW9uIn19 Accessed 05 Oct 2022

Jaimes Y, Aranzazu F (2010) Manejo de las enfermedades del cacao (*Theobroma cacao* L) en Colombia, con énfasis en Monillia *(Moniliophthora roreri)*. ed. Colombia (Col): L. M. Calle. https://www.researchgate.net/publication/322776193_Manejo_de_las_enfermedades_del_cacao_Theobroma_cacao_L_en_Colombia_con_enfasis_en_monilia_Moniliophthora_roreri. Accessed 18 May 2023

Johnson JA, Harrington TC, Engelbrecht CJB (2005) Phylogeny and taxonomy of the north American clade of the *Ceratocystis fimbriata* complex. Mycologia 97(5):1067–1092. https://doi.org/10.3852/mycologia.97.5.1067

Jollife IT, Cadima J (2016) Principal component analysis: a review and recent developments. Phil Trans R Soc 374:20150202. https://doi.org/10.1098/rsta.2015.0202

Kanzi AM, Trollip C, Wingfield MJ, Barnes I, Van Der Nest MA, Wingfield BD (2020) Phylogenomic incongruence in *Ceratocystis*: a clue to speciation? BMC Genom 21(1). https://doi.org/10.1186/s12864-020-6772-0

Kassambara A, Mundt F (2020) Factoextra: Extract and Visualize the Results of Multivariate Data Analyses. R Package Version 1.0.7. https://CRAN.R-project.org/package=factoextra. Accessed 12 May 2022

Katoh K, Rozewicki J, Yamada KD (2018) MAFFT online service: multiple sequence alignment, interactive sequence choice and visualization. Brief Bioinf 20(4):1160–1166. https://doi.org/10.1093/bib/bbx108

Kouakou K, Kébé BI, Kouassi N, Aké S, Cilas C, Muller E (2012) Geographical distribution of Cacao swollen shoot virus Molecular Variability in Côte d'Ivoire. Plant Dis 96(10):1445–1450. https://doi.org/10.1094/PDIS-09-11-0749-RE

Kück P, Longo GC (2014) FASconCAT-G: extensive functions for multiple sequence alignment preparations concerning phylogenetic studies. Front Zool 11(1):81. https://doi.org/10.1186/s12983-014-0081-x

Lê S, Josse J, Rennes A, Husson F (2008) FactoMineR: an R Package for Multivariate Analysis. J Stat Softw 25(1). https://doi.org/10.18637/jss.v025.i01

Liu FF, Barnes I, Roux J, Wingfield MJ, Chen SF (2018) Molecular phylogenetics and microsatellite analysis reveal a new pathogenic *Ceratocystis* species in the asian-australian clade. Plant Pathol 67(5):1097–1113. https://doi.org/10.1111/ppa.12820

Lloren R (2023) Unveiling *Ceratocystis wilt* disease: a review of cocoa's unforgiving foe. IOP Conf Ser: Earth Environ Sci 1263:012008. https://doi.org/10.1088/1755-1315/1263/1/012008

Magalhães DM, Luz ED, Lopes UV, Niella AR, Damaceno VO (2016) Leaf disc method for screening *Ceratocystis* wilt resistance in cacao. Trop Plant Pathol 41(3):155–161. https://doi.org/10.1007/s40858-016-0081-9

Marelli JP, Guest DI, Bailey BA, Evans HC, Brown JK, Junaid M, Barreto RW, Lisboa DO, Puig AS (2019) Chocolate under threat from old and new cacao diseases. Phytopathol 109(8):1331–1343. https://doi.org/10.1094/PHYTO-12-18-0477-RVW

Marin M, Wingfield MJ (2006) A review of Ceratocystis Sensu stricto with special reference to the species complexes C. coerulescens and C. Fimbriata. Rev Fac Nac Agron Medellín 59(1):3045–3075. https://revistas.unal.edu.co/index.php/refame/article/view/24262 Accessed 5 Oct 2022

Marin M, Castro B, Gaitan A, Preisig O, Wingfield BD, Wingfield MJ (2003) Relationships of *Ceratocystis fimbriata* isolates from Colombian coffee-growing regions based on molecular data and pathogenicity. J Phytopathol 151(7–8):395–405. https://doi.org/10.1046/j.1439-0434.2003.00738.x

Marincowitz S, Barnes I, de Beer ZW, Wingfield MJ (2020) Epitypification of *Ceratocystis fimbriata*. Fung Syst Evol 6:289–298. https://doi.org/10.3114/fuse.2020.06.14

MADR-Ministerio de Agricultura y Desarrollo Rural (2019) Cadena de Cacao. Dirección de Cadenas Agrícolas y Forestales. p 7

Mota-Gutierrez J, Botta C, Ferrocino I, Giordano M, Bertolino M, Dolci P, Cannoni M, Cocolin L (2018) Dynamics and biodiversity of bacterial and yeast communities during fermentation of cocoa beans. Appl Environ Microbiol 84(19). https://doi.org/10.1128/AEM.01164-18

Muller E, Sackey S (2004) Molecular variability analysis of five new complete cacao swollen shoot virus genomic sequences. Arch Virol 150:53–66. https://doi.org/10.1007/s00705-004-0394-8

Oliveira LS, Guimarães LM, Ferreira MA, Nunes AS, Pimenta LV, Alfenas AC (2015) Aggressiveness, cultural characteristics, and genetic variation of *Ceratocystis fimbriata* on *Eucalyptus* spp. Pathol 45(6):505–514. https://doi.org/10.1111/efp.12200

Oliveira LS, Harrington TC, Ferreira MA, Damacena MB, Al-Sadi AM, Al-Mahmooli IH, Alfenas AC (2015b) Species or genotypes? Reassessment of four recently described species of the Ceratocystis wilt pathogen, Ceratocystis fimbriata, on Mangifera indica. Phytopathology 105(9):1229–1244. https://doi.org/10.1094/PHYTO-03-15-0065-R

Paladines-Rezabala A, Moreira-Morrillo A, Mieles AE, Garcés-Fiallos FR (2022) Advances in understanding of the interaction between *Ceratocystis cacaofunesta* and *Xyleborus ferrugineus* (Coleoptera: Curculionidae: Scolytinae) on cocoa trees. Sci Agropecu 13(1):43–52. https://doi.org/10.17268/sci.agropecu.2022.004

Pantone Colour Finder https://www.pantone.com/color-finder#/pick?pantoneBook=pantoneSolidCoatedV3M2. Accessed 08 Agu 2022

Pinheiro J, Bates D, DebRoy S, Sarkar DR (2022) nlme: Linear and Nonlinear Mixed Effects Models. R package version 3.1–155. https://cran.rproject.org/package=nlme. Accessed 12 May 2022

Procter JB, Carstairs GM, Soares B, Mourão K, Ofoegbu TC, Barton D, Lui L, Menard A, Sherstnev N, Roldan-Martinez D, Duce S, Martin DM, Barton GJ (2021) Alignment of biological sequences with Jalview. Methods Mol Biol 2231:203–224. https://doi.org/10.1007/978-1-0716-1036-7_13

Quang-Minh B, Lanfear R, Ly-Trong Jana, Trifinopoulos N, Schrempf D, Schmidt HA (2022) IQ-TREE version 2.2.0: Tutorials and Manual Phylogenomic software by maximum likelihood. http://www.iqtree.org. Accessed 10 Apr 2023

Quinlan AR (2014) BEDTools: the swiss-Army tool for genome feature analysis. Curr Protoc Bioinform 47. 11.12.1-11.12.34

Rambaut A (2018) FigTree v 1.4.4: tree figure drawing tool. http://tree.bio.ed.ac.uk/software/figtree/. Accessed 20 Apr 2023

Reyes BM, Fonseca PL, Heming NM, Conceição LB, Nascimento KT, Gramacho KP, Arevalo-Gardini E, Pirovani CP, Aguiar ER (2023) Characterization of the microbiota dynamics associated with *Moniliophthora Roreri*, causal agent of cocoa frosty pod rot disease, reveals new viral species. Front Microbiol 3(13):1053562. https://doi.org/10.3389/fmicb.2022.1053562

Rodas CA, Van Wyk M, Wingfield BD, Wingfield MJ, Van Wyk J, Wingfield M (2008) *Ceratocystis neglecta sp. nov*., infecting Eucalyptus trees in Colombia. Fungal Divers. 28: 73–84. https://www.researchgate.net/publication/215735986_Ceratocystis_neglecta_sp_nov_infecting_Eucalyptus_trees_in_Colombia. Accessed 18 May 2023

Rodríguez-Polanco E, Morales JG, Muñoz-Agudelo M, Segura JD, Carrero ML (2020) Morphological, molecular, and pathogenic characterization of *phytophthora palmivora* isolates causing black pod rot of cacao in Colombia. Span J Agric Res 18(2):1–15. https://doi.org/10.5424/sjar/2020182-15147

Ronquist F, Huelsenbeck JP, Teslenko M, Zhang C, Nylander JA (2020) MrBayes version 3.2 Manual: Tutorials and Model Summaries. https://gensoft.pasteur.fr/docs/mrbayes/3.2.7/Manual_MrBayes_v3.2.pdf. Accessed 27 Apr 2023

Santos PL, Firmino AC, Tozze HJ, de Barros SA, Furtado EL (2011) In vitro *Ceratocystis* sp. behavior under differents temperatures, culture medium and pH. Revista Eletrônica de Educação e Ciência. 1(1): 07–17. https://www.fira.edu.br/revista/ano1_num1_ed1_art2_pag7.pdf. Accessed 12 May 2022

Singh BK, Delgado-Baquerizo M, Egidi E, Guirado E, Leach JE, Liu H, Trivedi P (2023) Climate change impacts on plant pathogens, food security and paths forward. Nat Rev Microbiol 21640–656. https://doi.org/10.1038/s41579-023-00900-7

Suwandi S, Irsan C, Hamidson H, Umayah A, Asriyani KD (2021) Identification and characterization of *Ceratocystis fimbriata* causing lethal wilt on the lansium tree in Indonesia. Plant Pathol J 37(2):124–136. https://doi.org/10.5423/PPJ.OA.08.2020.0147

Ten Hoppen GM, Deberdt P, Mbenoun M, Cilas C (2012) Modelling cacao pod growth: implications for disease control. Ann Appl Biol 160(3):260–272. https://doi.org/10.1111/j.1744-7348.2012.00539.x

Tumura KG, Edson P, Furtado L (2012) Murcha Por *Ceratocystis* em eucalipto: avaliação de resistência e análise epidemiológica. Summa Phytopathol 38(1). https://doi.org/10.1590/S0100-54052012000100009

Valdetaro DC, Oliveira LS, Guimarães LM, Harrington TC, Ferreira MA, Freitas RG, Alfenas AC (2015) Genetic variation, morphology, and pathogenicity of *Ceratocystis fimbriata* on *Hevea brasiliensis* in Brazil. Trop Plant Pathol 40(3):184–192. https://doi.org/10.1007/s40858-015-0036-6

Van Wyk M, Wingfield BD, Marin M, Wingfield MJ (2010) New *Ceratocystis* species infecting coffee, cacao, citrus, and native trees in Colombia. Fungal Divers 40:103–117. https://doi.org/10.1007/s13225-009-0005-9

Ward JH (1963) Hierarchical grouping to optimize an objective function. J Am Stat Assoc 58(301):236–244. https://doi.org/10.1080/01621459.1963.10500845

Wyk M, Van Wingfield BD, Al-Adawi AO, Rossetto CJ, Ito MF, Wingfield MJ (2011) Two new *Ceratocystis* species associated with mango disease in Brazil. Mycotaxon 117:381–404. https://doi.org/10.5248/117.381

Xu K, Li J, Yang X, Zhang R, Li X, Xie M, Huang Q (2020) Postharvest rot on carrot caused by *Ceratocystis fimbriata* and *Chalaropsis thielavioides* (≡ *Thielaviopsis thielavioides*) in China. J Gen Plant Pathol 86(4):322–325. https://doi.org/10.1007/s10327-020-00919-1